

## Chalcone Derivatives as Corrosion Inhibitors for Carbon Steel in 1 M HCl Solutions

A.S. Fouda<sup>1,\*</sup>, K. Shalabi<sup>1</sup>, G.Y. Elewady<sup>1</sup> and H.F. Merayyed<sup>2</sup>

<sup>1</sup>Department of Chemistry, Faculty of Science, Mansoura University, Mansoura-35516, Egypt

<sup>2</sup>Department of Chemistry, Faculty of Science, Omar Al-mukhtar University, Albayda, Libya

\*E-mail: [asfouda@hotmail.com](mailto:asfouda@hotmail.com)

Received: 19 April 2014 / Accepted: 17 July 2014 / Published: 29 September 2014

---

The effect of some chalcone derivatives on the dissolution of carbon steel in 1.0 M HCl solution was studied using weight loss, potentiodynamic polarization measurements, electrochemical impedance spectroscopy (EIS) and electrochemical frequency modulation (EFM) techniques. The inhibition efficiency was found to increase with increasing concentration of the inhibitors and decrease with raising temperature. The adsorption of chalcone derivatives on the carbon steel surface obeys the Langmuir adsorption isotherm. Polarization studies indicate that these investigated compounds are mixed type inhibitors. The thermodynamic functions of adsorption processes were calculated from weight loss at different temperatures data and were used to analyse the inhibitor mechanism. The surface morphology of the carbon steel specimens was evaluated using scanning electron microscope (SEM) and energy dispersive X-ray (EDX) analysis.

---

**Keywords:** Carbon steel, Corrosion inhibition, Chalcone derivatives, HCl, Potentiodynamic polarization, EIS, EFM, SEM, EDX.

### 1. INTRODUCTION

Evaluation of corrosion inhibitors for steel in acidic media is important for some industrial facilities as well as is very interesting from theoretical aspects. Carbon steel is an alloy of iron, which undergoes corrosion easily in acidic medium. Acidic solutions are extensively used in chemical laboratories and in several industrial processes such as acid pickling, acid cleaning, acid descaling and oil wet cleaning, etc. Also carbon steel is used under different conditions in chemical and allied industries for handling alkaline, acid and salt solutions [1]. The organic compounds adsorb on metallic surface and then decrease the corrosion rate [2-4]. It has been observed that adsorption depends mainly on certain physico-chemical properties of the inhibitor group, like functional groups, electron density

at the donor atom,  $\pi$ -orbital character, and the electronic structure of the molecule [5-10]. In general, organic compounds with oxygen, sulfur, and/or nitrogen as polar groups and conjugated double bonds in their structures have been reported to be good corrosion inhibitors for many metals and alloys in corrosive media [11-27]. The inhibiting action of these organic compounds is usually attributed to their interactions with the metallic surfaces via their adsorption. Polar functional groups are regarded as the reaction centre that stabilizes the adsorption process [23]. However, the adsorption of an inhibitor on a metal surface depends on a few factors, such as the nature and surface charge of the metal, the adsorption mode, the inhibitor's chemical structure, and the type of the electrolyte solution [28].

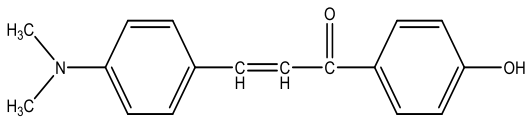
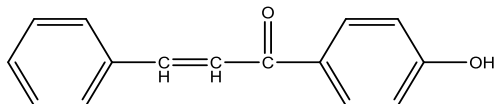
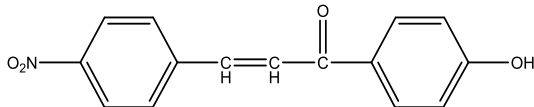
The objective of this study is to investigate the corrosion behavior of carbon steel in 1.0 M HCl at different temperatures in the presence of some chalcone derivatives using chemical and electrochemical techniques. The surface morphology of the carbon steel specimens was evaluated using SEM and EDX analysis.

## 2. EXPERIMENTAL

### 2.1. Materials and solutions

Carbon steel strips (BDH grade) containing (weight %): 0.2 C, 0.024 P, 0.003 Si, 0.35 Mn, and rest Fe were used in this investigation. All chemicals used were of AR grade. Specimens of C-steel strips were abraded successively by emery papers of different grades, i.e. 320, 400, 600, 800 and 1000 finally abraded with a 4/0 emery paper to obtain mirror like finish, then degreased ultrasonically with ethyl alcohol and rinsed with bidistilled water several times and dried between two fitter papers. AR grade hydrochloric acid (37 %) was used for preparing the corrosive solutions.

Appropriate concentration of aggressive solutions used (1.0 M HCl) was prepared by dilution using bidistilled water. The structures of the investigated compounds are shown below [29]:

Name	Structure	Chemical formula & Molecular weight
1 3-(4-(dimethylamino)phenyl)-1-(4-hydroxyphenyl)prop-2-en-1-one		$C_{17}H_{17}NO_2$ 267.32
2 1-(4-hydroxyphenyl)-3-phenylprop-2-en-1-one		$C_{15}H_{12}O_2$ 224.25
3 1-(4-hydroxyphenyl)-3-(4-nitrophenyl)prop-2-en-1-one		$C_{15}H_{11}NO_4$ 269.25

## 2.2. Weight loss measurements

For weight loss measurements, rectangular C-steel specimens of size 20 x 20 x 2 mm were immersed in 100 ml inhibited and uninhibited solutions and allow to stand for several intervals at 25 ± 1°C in water thermostat. Therefore, the weight losses (W) given by:

$$W = (m_1 - m_2) \quad (1)$$

where  $m_1$  and  $m_2$  are the weights of metal before and after exposure to the corrosive solution, respectively. The percentage inhibition efficiency (% IE) and the degree of surface coverage ( $\theta$ ) of the investigated compounds were calculated from the following equation:

$$\%IE = \theta \times 100 = \left(1 - \frac{W_{(inh)}}{W_{(free)}}\right) \times 100 \quad (2)$$

where,  $W_{free}$  and  $W_{inh}$  are the weight loss in the absence and presence of inhibitor, respectively.

## 2.3. Electrochemical measurements

A three electrode electrochemical cell was used. The working electrode was C-steel of surface area of 1 cm<sup>2</sup>. Before each experiment, the electrode was abraded using emery papers as before. After this, the electrode was cleaned ultrasonically with ethyl alcohol and washed by bidistilled water. All potentials were given with reference to the saturated calomel electrode (SCE). The counter electrode was a platinum plate of surface area of 1 cm<sup>2</sup>. The working electrode was immersed in the test solution during 30 min until a steady state open circuit potential ( $E_{ocp}$ ) was obtained. The polarization curves were recorded by polarization from -0.6 V to 0.2 V under potentiodynamic conditions corresponding to 1 mV/s (sweep rate) and under air atmosphere. All measurements were carried out with C-steel electrode in 1.0 M HCl in the absence and presence of different concentrations ( $1 \times 10^{-6}$  –  $11 \times 10^{-6}$  M) of the investigated compounds at 25°C. The inhibition efficiency (% IE) and surface coverage ( $\theta$ ) were calculated from equation (3):

$$\%IE = \theta \times 100 = \left(1 - \frac{i_{corr(inh)}}{i_{corr(free)}}\right) \times 100 \quad (3)$$

where  $i_{corr(free)}$  and  $i_{corr(inh)}$  are the corrosion current densities in the absence and presence of inhibitor, respectively.

Electrochemical impedance spectroscopy measurements were performed using the same cell that used in polarization experiments. The EIS carried out over a frequency range of 1 Hz to 100 kHz, with a signal amplitude perturbation of 10 mV. The inhibition efficiency (% IE) and surface coverage ( $\theta$ ) of the investigated compounds obtained was calculated from equation (4):

$$\%IE = \theta \times 100 = \left(1 - \left[\frac{R_{ct}^0}{R_{ct}}\right]\right) \times 100 \quad (4)$$

where  $R_{ct}^0$  and  $R_{ct}$  are the charge transfer resistance values in the absence and presence of the inhibitors, respectively.

Electrochemical frequency modulation is a non-destructive technique as electrochemical impedance spectroscopy that can directly and rapidly give values of the corrosion current without a prior knowledge of Tafel constants. The great of the EFM is the causality factors, which serves as an internal check on the validity of the EFM measurement. With the causality factors the experimental

EFM data can be verified [30, 31]. Identical cell assembly was used as in impedance studies. All electrochemical measurements were carried out using Potentiostat /Galvanostat / Zra analyzer (Gamry PCI4-G750). A personal computer with DC105 software for potentiodynamic, EIS300 software for EIS and EFM140 software for EMF and Echem Analyst v 5.21 was used for data fitting.

2.4. Surface examination

The specimens of carbon steel used for surface morphology examination were immersed in 1.0 M HCl in the absence (blank) and presence of  $11 \times 10^{-6}$  M of investigated compounds at 25 °C for 24 hours. The analysis was performed using scanning electron microscope (JEOL JSM-5500, Japan). Rough elemental analyses for the exposed surface were conducted by EDX technique.

3. RESULTS AND DISCUSSION

3.1. Weight loss measurements

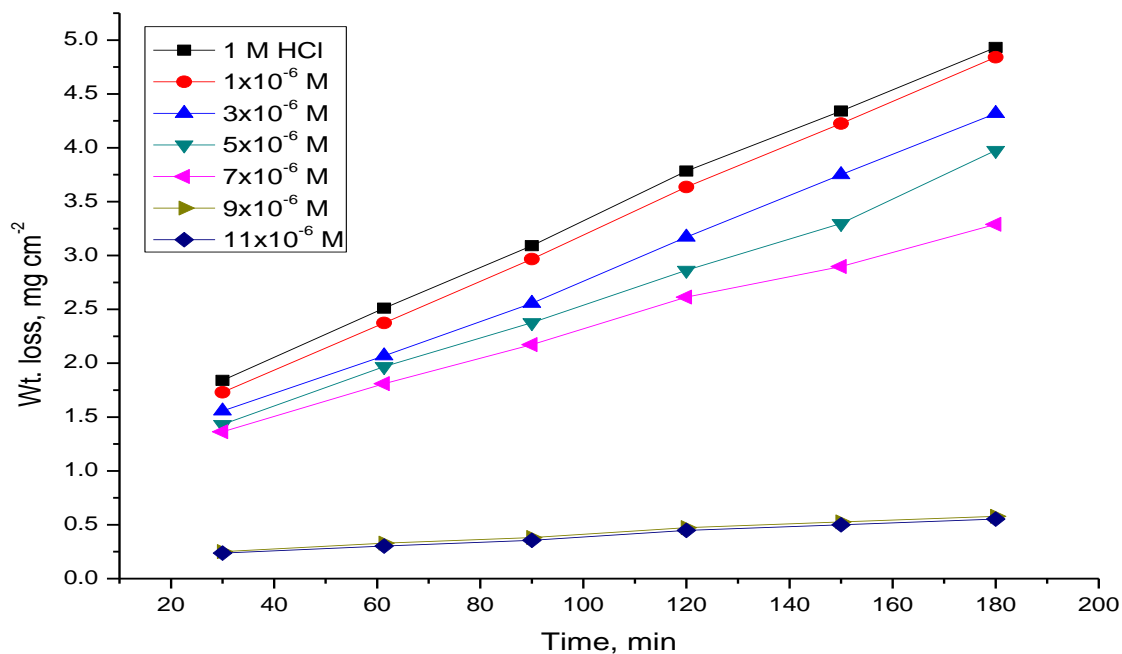


Figure 1. Weight loss-time curves for the corrosion of C-steel in 1.0 M HCl in the absence and presence of different concentrations of compound (1) at 25°C

Figure 1 shows the effect of concentration of compound (1) on the weight loss vs. time of C-steel at 25°C. Similar curves were obtained for the other two compounds (not shown). It is obvious that the weight loss of C-steel in presence of inhibitors varies linearly with time, and is much lower than that obtained in blank solution. The linearity obtained indicated the absence of insoluble surface film

during corrosion and that the inhibitors were first adsorbed onto the metal surface and, therefore, impede the corrosion process [32].

The calculated values of the percentage inhibition efficiency (% IE) at different concentrations of chalcone derivatives in 1.0 M HCl at different temperatures (25- 45°C) are given in Tables 1, 2. From these Tables, the inhibition efficiency increases by increasing the concentrations of chalcone derivatives and decreases by raising the temperature. This behavior could be attributed to the increase of the number of adsorbed molecules at the metal surface and by raising the temperature desorption of inhibitor molecules from the metal surface will takes place. At one and the same inhibitor concentration % IE decreases in the following order: (1) > (2) > (3).

**Table 1.** Corrosion rate (C.R.) in ( $\text{mg cm}^{-2} \text{min}^{-1}$ ) and inhibition efficiency data obtained from weight loss measurements for carbon steel in 1.0 M HCl solution in the absence and presence of different concentrations of investigated compounds at 25°C

Compound	Conc., x 10 <sup>-6</sup> M	Corrosion Rate (CR), mg cm <sup>-2</sup> min <sup>-1</sup>	$\theta$	% IE
<b>1 M HCl</b>		0.0500	----	----
<b>1</b>	1	0.0220	0.56	56
	3	0.0199	0.602	60.2
	5	0.0183	0.634	63.4
	7	0.0177	0.646	64.6
	9	0.0032	0.936	93.6
	11	0.0023	0.954	95.4
<b>2</b>	1	0.0303	0.394	39.4
	3	0.0264	0.472	47.2
	5	0.0239	0.522	52.2
	7	0.0218	0.564	56.4
	9	0.0039	0.922	92.2
	11	0.0037	0.926	92.6
<b>3</b>	1	0.0301	0.398	39.8
	3	0.0276	0.448	44.8
	5	0.0268	0.464	46.4
	7	0.0201	0.598	59.8
	9	0.0041	0.918	91.8
	11	0.0038	0.924	92.4

**Table 2.** Data of weight loss measurements for carbon steel in 1 M HCl solution in the absence and presence of different concentrations of investigated inhibitors at 30–45°C

Compound	Conc., x 10 <sup>-6</sup> , M	30°C		35°C		40°C		45°C	
		θ	% IE						
<b>1</b>	1	0.229	22.9	0.144	14.4	0.117	11.7	0.104	10.4
	3	0.504	50.4	0.393	39.3	0.326	32.6	0.312	31.2
	5	0.651	65.1	0.526	52.6	0.496	49.6	0.477	47.7
	7	0.733	73.3	0.669	66.9	0.641	64.1	0.636	63.6
	9	0.858	85.8	0.794	79.4	0.776	77.6	0.772	77.2
	11	0.915	91.5	0.909	90.9	0.897	89.7	0.876	87.6
<b>2</b>	1	0.278	27.8	0.237	23.7	0.221	22.1	0.122	12.2
	3	0.532	53.2	0.471	47.1	0.455	45.5	0.248	24.8
	5	0.705	70.5	0.602	60.2	0.549	54.9	0.343	34.3
	7	0.772	77.2	0.662	66.2	0.602	60.2	0.394	39.4
	9	0.842	84.2	0.713	71.3	0.638	63.8	0.424	42.4
	11	0.859	85.9	0.754	75.4	0.663	66.3	0.456	45.6
<b>3</b>	1	0.393	39.3	0.280	28.0	0.162	16.2	0.128	12.8
	3	0.682	68.2	0.597	59.7	0.414	41.4	0.348	34.8
	5	0.811	81.1	0.740	74.0	0.579	57.9	0.507	50.7
	7	0.854	85.4	0.806	80.6	0.713	71.3	0.624	62.4
	9	0.891	89.1	0.873	87.3	0.796	79.6	0.721	72.1
	11	0.924	92.4	0.904	90.4	0.865	86.5	0.807	80.7

### 3.2 Adsorption isotherm

Basic information on the interaction between the inhibitors and the C-steel can be provided by the adsorption isotherm. Two main types of interactions can describe the adsorption of the organic compound: physical adsorption and chemical adsorption. These are influenced by the chemical structure of the inhibitor, the type of the electrolyte, the charge and nature of the metal. The surface coverage, θ, of the metal surface by the adsorbed inhibitor was evaluated from weight loss measurements using equation (2). The θ values of different inhibitor concentrations at 25 °C were tested by fitting to various isotherms including, Frumkin, Langmuir, Temkin and Flory-Huggins. By far the best fit was obtained with the Langmuir isotherm is given as [33]:

$$\frac{C}{\theta} = \frac{1}{K_{ads}} + C \tag{5}$$

where C is the inhibitor concentration and K<sub>ads</sub> is the equilibrium constant of adsorption process.

A plot of (C /θ) against C, for all concentrations of inhibitors (Figure 2) a straight line relationship was obtained in all cases with correlation coefficients (R<sup>2</sup>) in more than 0.994. The standard free energy of adsorption ΔG°<sub>ads</sub> can be calculated from Eq. (6):

$$K_{ads} = \frac{1}{55.5} e^{\frac{-\Delta G_{ads}^{\circ}}{RT}} \tag{6}$$

The value of 55.5 is the concentration of water in solution expressed in mole per liter, R is the universal gas constant and T is the absolute temperature .

The deviation of the slope from unity as observed from this study could be interpreted that there are interactions between adsorbed species on the metal surface as well as changes in adsorption heat with increasing surface coverage [34, 35], factors that were ignored in the derivation of Langmuir isotherm. The negative  $\Delta G^{\circ}_{ads}$  values (Table 3) are consistent with the spontaneity of the adsorption process and the stability of the adsorbed layer on the C-steel surface [36].

It is generally accepted that the values of  $\Delta G^{\circ}_{ads}$  up to  $-20 \text{ kJ mol}^{-1}$  the types of adsorption were regarded as physisorption, the inhibition acts due to the electrostatic interaction between the charged molecules and the charged metal, while the values around  $-40 \text{ kJ mol}^{-1}$  or larger, were seen as chemisorption, which is due to the charge sharing or a transfer from the inhibitor molecules to the metal surface to form covalent bond [37, 38]. The  $\Delta G^{\circ}_{ads}$  values obtained in this study range from  $-36.2$  to  $-36.7 \text{ kJ mol}^{-1}$ . It suggested that the adsorption mechanism of investigated inhibitors on C-steel in 1.0 M HCl solution was typical of physisorption and chemisorption (mixed one).

Moreover, the adsorption heat can be calculated according to the Van't Hoff equation (7) [39]:

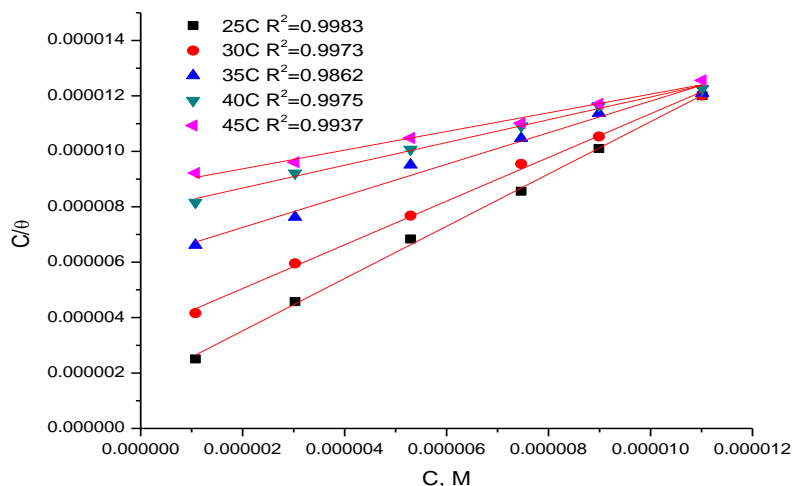
$$\ln K = -\frac{\Delta H^{\circ}_{ads}}{RT} + const \tag{7}$$

Figure 3 shows the plot of  $\log K_{ads}$  vs.  $1/T$  for carbon steel dissolution in 1.0 M HCl in the presence of chalcone derivatives. The  $\Delta H^{\circ}_{ads}$  values (Table 3) are negative, which show that the adsorption is an exothermic process [40].

Finally, the standard adsorption entropy  $\Delta S^{\circ}_{ads}$  can be calculated by the equation (8):

$$\Delta S^{\circ}_{ads} = \frac{\Delta H^{\circ}_{ads} - \Delta G^{\circ}_{ads}}{T} \tag{8}$$

The  $\Delta S^{\circ}_{ads}$  values (Table 3) are negative, which show that the adsorption is an exothermic process and always accompanied by a decrease of entropy. The reason can be explained as follows: the adsorption of organic inhibitor molecules from the aqueous solution. Table 3 lists all the above calculated thermodynamic parameters [41-42].



**Figure 2.** Langmuir adsorption isotherm of compound (1) on C-steel surface in 1.0 M HCl at different temperatures

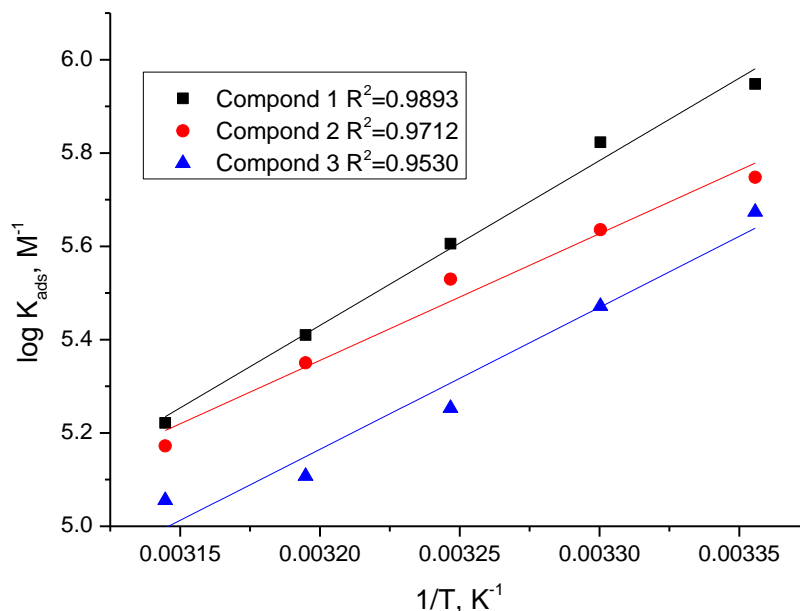


**Figure 3.** Log  $K_{ads}$  vs.  $(1/T)$  curves for carbon steel dissolution in 1.0 M HCl in the presence of chalcone derivatives

**Table 3.** Thermodynamic parameters for the adsorption of three compounds on carbon steel surface in 1 M HCl at different temperatures

Compounds	Temp., K	$K_{ads} \times 10^4, M^{-1}$	$-\Delta G_{ads}^{\circ}, kJ mol^{-1}$	$-\Delta H_{ads}^{\circ}, kJ mol^{-1}$	$-\Delta S_{ads}^{\circ}, J mol^{-1} K^{-1}$
<b>I</b>	298	88.73	43.89	76.54	<b>109.56</b>
	303	66.56	43.90		<b>107.72</b>
	308	40.33	43.34		<b>107.78</b>
	313	18.88	42.07		<b>110.12</b>
	318	14.66	42.08		<b>108.38</b>
	298	60.21	42.93	64.36	<b>71.91</b>
	303	29.64	41.86		<b>74.24</b>
	308	16.27	41.02		<b>75.78</b>
	313	12.81	41.06		<b>74.43</b>
	318	12.04	41.56		<b>71.71</b>
<b>III</b>	298	55.97	42.75	45.73	<b>10.00</b>
	303	43.21	42.81		<b>9.62</b>
	308	33.87	42.90		<b>9.20</b>
	313	33.17	43.54		<b>7.00</b>
	318	14.86	42.11		<b>11.38</b>

### 3.3 Kinetic-thermodynamic corrosion parameters

As noticed previously, the adsorption process was well elucidating by using a thermodynamic model, in addition a kinetic-thermodynamic model was another tool to explain the mechanism of corrosion inhibition for an inhibitor. The apparent effective activation energies ( $E_a^*$ ) for the corrosion

reaction of C-steel in HCl in the absence and presence of different concentrations of investigated compounds were calculated from Arrhenius-type equation (9) [43]:

$$\text{Rate (k)} = A e^{\frac{-E_a^*}{RT}} \tag{9}$$

where A is the Arrhenius pre-exponential factor. A plot of log k (corrosion rate) vs. 1 / T gave straight lines as shown in (Figure 4). The entropy of activation ( $\Delta S^*$ ) and the enthalpy of activation ( $\Delta H^*$ ) for the intermediate complex in the transition state for the corrosion of C-steel in HCl in the absence and presence of different concentrations of investigated compounds were obtained by applying the transition-state equation (10) [44-46]:

$$\text{Rate (k)} = \frac{RT}{Nh} e^{\frac{\Delta S^*}{R}} e^{\frac{-\Delta H^*}{RT}} \tag{10}$$

where h is the Planck's constant and N is the Avogadro's number.

A plot of log k (corrosion rate) / T vs. 1 / T should give a straight lines (Figure 5), with a slope of  $(-\Delta H^* / 2.303R)$ , and an intercept of  $[(\log( RT / Nh ) + (\Delta S^*/2.303R)]$  [47,48], from which the values of  $\Delta H^*$  and  $\Delta S^*$  were calculated, respectively. (Table 4) exhibited values of apparent activation energy, apparent enthalpies  $\Delta H^*$  and entropies  $\Delta S^*$  for C-steel dissolution in 1.0 M HCl solution in the absence and presence of different investigated compounds. The presence of inhibitors increased the activation energies of C-steel indicating strong adsorption of the inhibitor molecules on the metal surface and the presence of these additives induces the adsorption of these additives on the surface of C-steel. Values of the entropy of activation  $\Delta S^*$  in the absence and in presence of the studied compounds are negative. This implies that the activated complex in the rate determining step represents an association rather than a dissociation step [49]. This means that the activated molecules were in higher order state than that at the initial stage [50, 51].

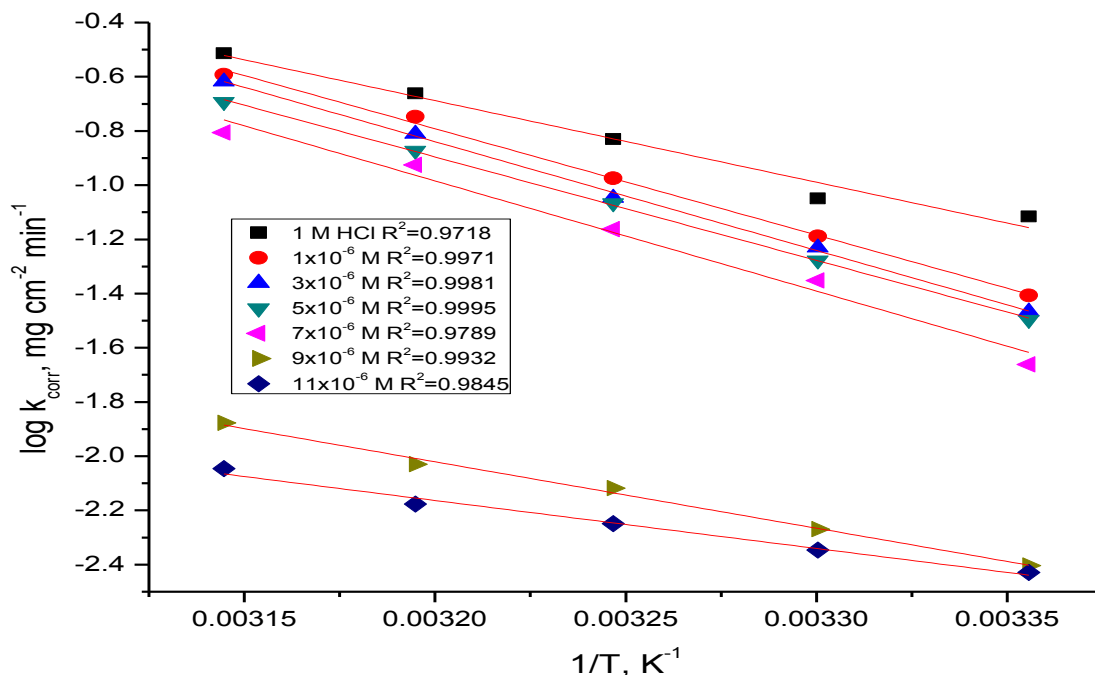


**Figure 4.** Arrhenius plots for C-steel corrosion rates ( $k_{\text{corr}}$ ) after 120 minutes of immersion in 1.0 M HCl in the absence and presence of different concentrations of compound (1)

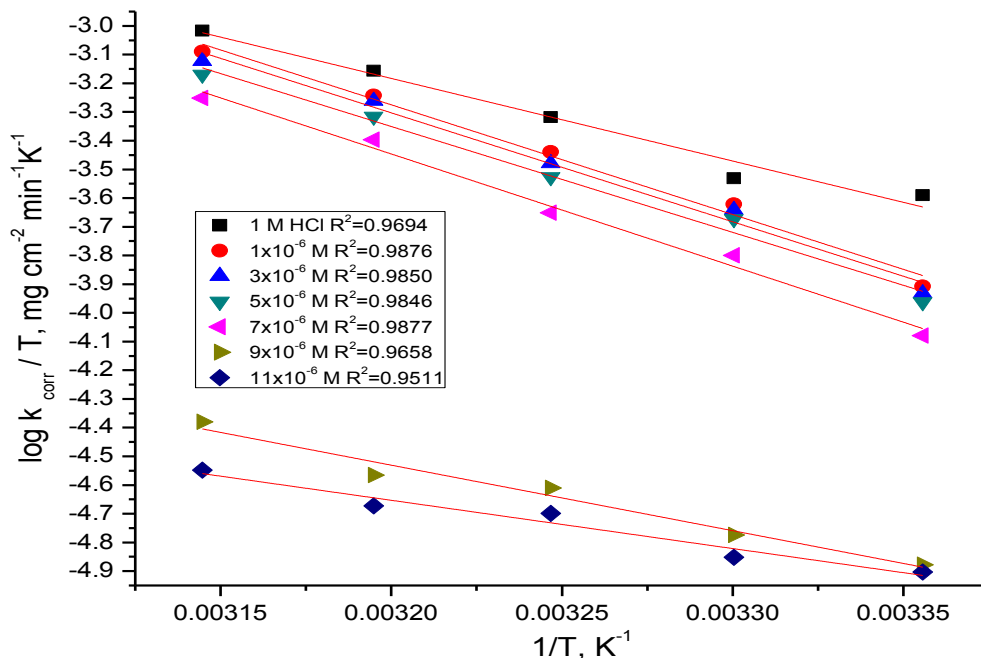


**Figure 5.** Plots of ( $\log k_{\text{corr}}$ ) vs.  $1/T$  for corrosion of C-steel in 1.0 M HCl in the absence and presence of different concentrations of compound (1)

**Table 4.** Activation parameters for the dissolution of carbon steel in the presence and absence of different concentrations of inhibitors in 1.0 M HCl

Inhibitor	Conc., x 10 <sup>-6</sup> M	Activation parameters		
		E <sub>a</sub> <sup>*</sup>	ΔH <sup>*</sup>	-ΔS <sup>*</sup>
		kJ mol <sup>-1</sup>	kJ mol <sup>-1</sup>	J mol <sup>-1</sup> K <sup>-1</sup>
1 M HCl		56.40	23.93	82.16
1	1	97.86	41.38	42.30
	3	99.27	41.99	46.00
	5	101.36	42.90	52.39
	7	98.45	41.64	42.21
	9	39.79	16.17	167.62
	11	43.53	17.79	157.15
2	1	75.97	31.88	25.55
	3	78.50	32.97	18.30
	5	73.98	31.01	33.86
	7	76.05	31.91	28.40
	9	44.76	18.33	149.32
	11	35.56	14.33	181.02
3	1	77.70	32.63	20.78
	3	75.71	31.76	28.24
	5	72.30	30.28	39.95
	7	81.95	34.47	10.42
	9	139.45	59.44	171.91
	11	140.93	60.08	173.83

### 3.4. Polarization Curves

Figure 6 illustrates the polarization curves of carbon steel in 1.0 M HCl solution without and with various concentrations of compound (1) at 25°C. The presence of investigated compounds shift both anodic and cathodic branches to the lower values of corrosion current densities and thus causes a remarkable decrease in the corrosion rate. The parameters derived from the polarization curves in (Figure 6) are given in Table 5. In 1.0 M HCl solution, the presence of the investigated compounds cause a remarkable decrease in the corrosion rate i.e., shifts both anodic and cathodic curves to lower current densities. In other words, both cathodic and anodic reactions of carbon steel electrode are retarded by the investigated compounds in HCl solutions. The Tafel slopes of  $\beta_a$  and  $\beta_c$  at 25°C do not change remarkably upon addition of the investigated compounds, which indicates that the presence of chalcone derivatives do not change the mechanism of hydrogen evolution and the metal dissolution process. Generally, an inhibitor can be classified as cathodic or anodic type if the shift of corrosion potential in the presence of the inhibitor is more than 85 mV with respect to that in the absence of the inhibitor [52, 53]. In the presence of chalcone derivatives,  $E_{\text{corr}}$  shifts to less negative but this shift is very small (about 20-30 mV), which indicates that chalcone derivatives can be arranged as a mixed-type inhibitor, with predominant anodic effectiveness. The % inhibition increased with increasing the concentration of the compounds, the inhibition efficiency of the three tested compounds measured by polarization method decreased in the following order: (1) > (2) > (3). This sequence is in accordance with that obtained from weight-loss measurements.

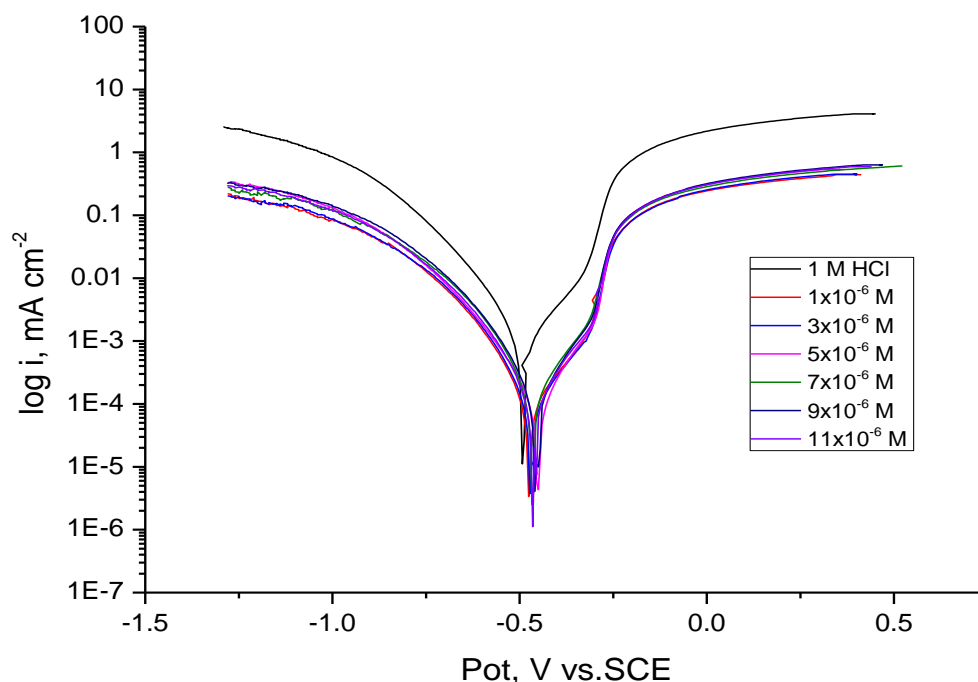


**Figure 6.** Potentiodynamic polarization curves for the corrosion of C-steel in 1.0 M HCl in the absence and presence of different concentrations of compound (1) at 25°C

**Table 5.** The effect of concentration of the investigated compounds on the free corrosion potential ( $E_{\text{corr}}$ ), corrosion current density ( $i_{\text{corr}}$ ), Tafel slopes ( $\beta_a$  &  $\beta_c$ ), corrosion rate (C.R.), degree of surface coverage ( $\theta$ ) and inhibition efficiency (% IE) for the corrosion of carbon steel 1.0 M HCl at 25 °C

Comp.	Conc., M	$i_{\text{corr}}$ , $\mu\text{A cm}^{-2}$	$-E_{\text{corr}}$ , mV(vs SCE)	$\beta_a$ , mV dec <sup>-1</sup>	$\beta_c$ , mV dec <sup>-1</sup>	C.R., mpy	$\theta$	% IE
Blank		488.0	492.00	105	111	222.70	--	--
1	$1 \times 10^{-6}$	160	475	184	141	96.31	0.668	66.8
	$3 \times 10^{-6}$	116	471	153	131	68.99	0.753	75.9
	$5 \times 10^{-6}$	104	452	116	131	55.40	0.784	78.4
	$7 \times 10^{-6}$	86.70	467	104	118	42.48	0.820	82.0
	$9 \times 10^{-6}$	64.10	458	99	115	29.22	0.869	86.9
	$11 \times 10^{-6}$	50.20	465	104	112	24.73	0.898	89.8
2	$1 \times 10^{-6}$	186	483	116	149	111.96	0.614	61.4
	$3 \times 10^{-6}$	146	465	84	139	86.83	0.697	69.7
	$5 \times 10^{-6}$	137	456	90	141	72.98	0.716	71.6
	$7 \times 10^{-6}$	101	459	85	154	49.49	0.791	79.0
	$9 \times 10^{-6}$	70.20	466	73	112	32.00	0.854	85.4
	$11 \times 10^{-6}$	54.30	466	84	128	24.78	0.887	88.7
3	$1 \times 10^{-6}$	248.0	472	152	198	149.28	0.492	49.2
	$3 \times 10^{-6}$	160.0	457	142	168	95.16	0.672	67.2
	$5 \times 10^{-6}$	148.0	452	132	168	78.83	0.697	69.7
	$7 \times 10^{-6}$	120.0	482	110	122	58.79	0.754	75.4
	$9 \times 10^{-6}$	90.0	468	99	101	41.03	0.816	81.6
	$11 \times 10^{-6}$	82.00	481	96	93	37.41	0.832	83.2

### 3.5. Electrochemical impedance spectroscopy (EIS)

Figures 7 and 8 show the Nyquist and Bode diagrams of carbon steel in 1.0 M HCl solutions containing different concentrations of compound (1) at 25°C. Similar curves were obtained for other compounds (not shown). All the impedance spectra exhibit one single depressed semicircle. The diameter of semicircle increases with the increase of the investigated compounds concentration. The impedance spectra exhibit one single capacitive loop, which indicates that the corrosion of steel is mainly controlled by a charge transfer process [54] and the presence of the investigated compounds does not change the mechanism of carbon steel dissolution [55]. In addition, these Nyquist diagrams are not perfect semicircles in 1.0 M HCl that can be attributed to the frequency dispersion effect as a result of the roughness and inhomogeneous of electrode surface [38]. Furthermore, the diameter of the capacitive loop in the presence of inhibitor is larger than that in the absence of inhibitor (blank solution), and increased with the inhibitor concentration. This indicates that the impedance of inhibited substrate increased with the inhibitor concentration. [56]. This behavior is usually attributed to the inhomogeneity of the metal surface arising from surface roughness or interfacial phenomena [57], which is typical for solid metal electrodes [58]. Generally, when a non-ideal frequency response is presented, it is commonly accepted to employ the distributed circuit elements in the equivalent circuits. What is most widely used is the constant phase element (CPE), which has a non-integer power dependence on the frequency [59]. Thus, the equivalent circuit depicted in Figure 9 is employed to

analyze the impedance spectra, where  $R_s$  represents the solution resistance,  $R_{ct}$  denotes the charge-transfer resistance, and a CPE instead of a pure capacitor represents the interfacial capacitance. The impedance of a CPE is described by the equation (11):

$$Z_{CPE} = Y_0^{-1}(j\omega_{max})^{-n} \quad (11)$$

where  $Y_0$  is the magnitude of the CPE,  $j$  is an imaginary number,  $\omega$  is the angular frequency at which the imaginary component of the impedance reaches its maximum values, and  $n$  is the deviation parameter of the CPE:  $-1 \leq n \leq 1$ . The values of the interfacial capacitance  $C_{dl}$  can be calculated from CPE parameter values  $Y_0$  and  $n$  using equation (12) [60]:

$$C_{dl} = Y_0(\omega_{max})^{n-1} \quad (12)$$

The values of the parameters such as  $R_s$ ,  $R_{ct}$ , through EIS fitting as well as the derived parameters  $C_{dl}$  and % IE are listed in Table 6. It is clear that the value of  $R_{ct}$  increases on increasing the concentration of the inhibitor, indicating that the corrosion rate decreases in the presence of the inhibitor. It is also clear that the value of  $C_{dl}$  decreases on the addition of inhibitors, indicating a decrease in the local dielectric constant and/or an increase in the thickness of the electrical double layer, suggesting the inhibitor molecules function by the formation of the protective layer at the metal surface [58]. The order of inhibition efficiency obtained from EIS measurements is as follows: (1) < (2) < (3). This sequence is in accordance with that obtained from weight-loss and polarization measurements.

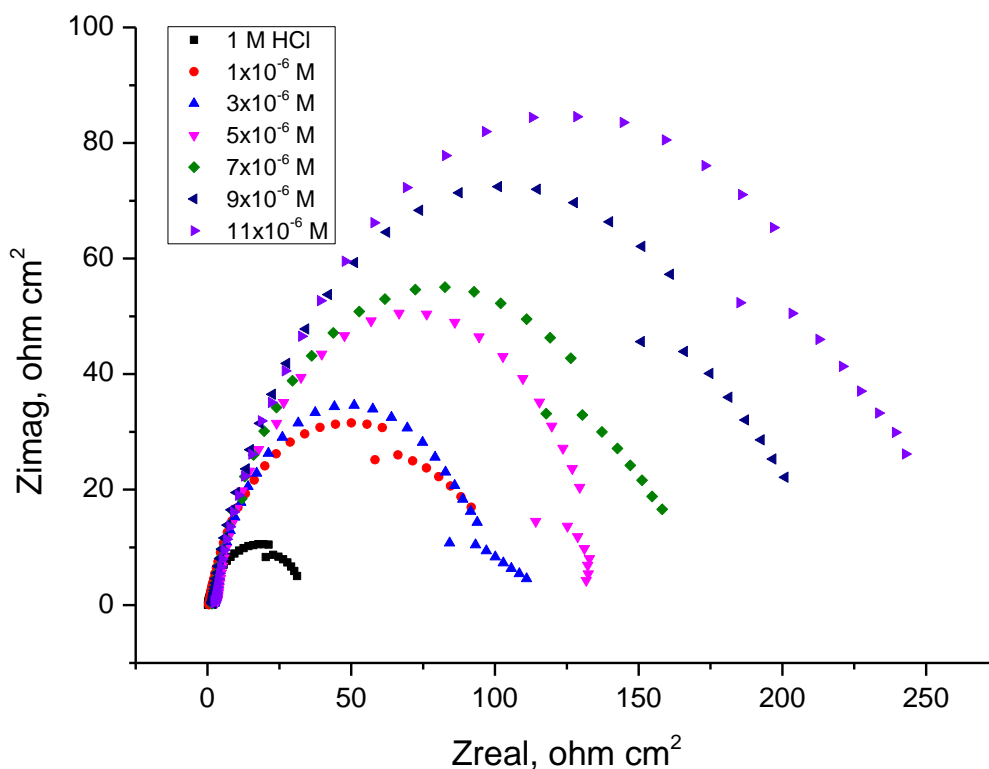


**Figure 7.** The Nyquist plots for corrosion of C-steel in 1.0 M HCl in the absence and presence of different concentrations of compound (1) at 25°C.

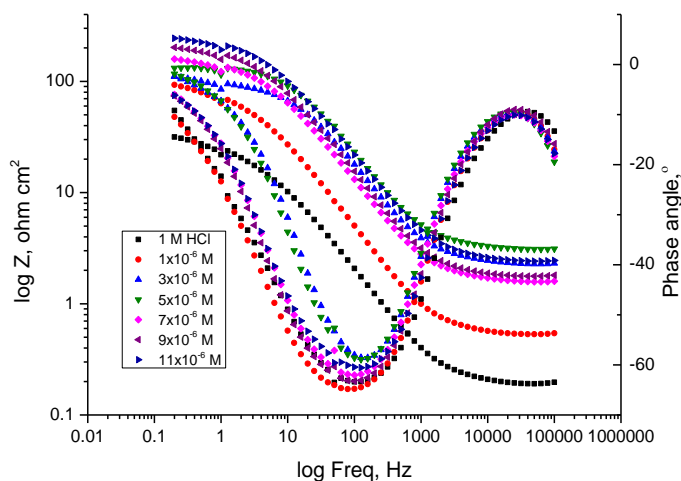


**Figure 8.** The Bode plots for corrosion of C-steel in 1.0 M HCl in the absence and presence of different concentrations of compound (1) at 25°C

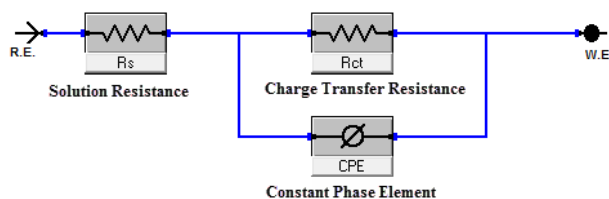


**Figure 9.** Equivalent circuit model used to fit experimental EIS

**Table 6.** Electrochemical kinetic parameters obtained by EIS technique for in 1 M HCl without and with various concentrations of investigated compounds at 25°C

Comp.	Conc., $\times 10^6$ M	$R_{ct}$ , $\Omega \text{ cm}^2$	$C_{dl}$ , $\mu\text{F cm}^{-2}$	$\theta$	%IE
Blank		30.23	1762.20	--	--
1	1	78.02	564.84	0.615	61.3
	3	101.7	488.09	0.703	70.3
	5	154.7	245.60	0.805	80.5
	7	187.7	230.55	0.839	83.9
	9	205.1	197.86	0.853	85.3
	11	289.8	152.74	0.896	89.6
2	1	77.69	471.74	0.611	61.1
	3	81.79	374.77	0.630	63.0
	5	102.9	341.38	0.706	70.6
	7	140.1	285.64	0.784	78.4
	9	202.7	69.91	0.851	85.1
	11	294.9	61.36	0.898	89.8
3	1	89.15	701.36	0.661	66.1
	3	97.98	334.36	0.692	69.2
	5	132.1	250.23	0.771	77.1
	7	153.9	239.52	0.804	80.4
	9	197.3	199.41	0.847	84.7
	11	240.3	151.18	0.874	87.4

### 3.6. Electrochemical frequency modulation technique (EFM)

The EFM is a nondestructive corrosion measurement technique that can directly give values of the corrosion current without prior knowledge of Tafel constants. Like EIS, it is a small AC signal. Intermodulation spectra obtained from EFM measurements of carbon steel in 1.0 M HCl solution, in the absence and presence of different concentrations of compound (1) at 25°C are presented in Figure 10. Each spectrum is a current response as a function of frequency.

The calculated corrosion kinetic parameters at different concentrations of the the investigated compounds in 1.0 M HCl at 25°C ( $i_{\text{corr}}$ ,  $\beta_a$ ,  $\beta_c$ , CF-2, CF-3 and %IE are given in Table 7. From this Table, the corrosion current densities decreased by increasing the concentration of investigated compounds, the inhibition efficiencies increase by increasing investigated compounds concentrations.

**Table 7.** Electrochemical kinetic parameters obtained by EFM technique for carbon steel in the absence and presence of various concentrations of inhibitors in 1.0 HCl at 25°C

Comp.	Conc., x 10 <sup>-6</sup> , M	$i_{\text{corr}}$ , $\mu\text{Acm}^{-2}$	$\beta_c$ $\text{mVdec}^{-1}$	$\beta_a$ $\text{mVdec}^{-1}$	CF-2	CF-3	CR mpy	$\theta$	%IE
Blank		423.3	293.8	126.2	2.009	3.983	193.3	-	-
1	1	152.1	366.4	141.3	2.046	3.894	75.06	0.6407	<b>64.07</b>
	3	121.9	155.3	132.5	2.411	2.741	60.15	0.7120	<b>71.20</b>
	5	81.01	131.9	117.8	2.050	2.203	39.98	0.8086	<b>80.86</b>
	7	50.55	137.6	133.5	1.265	2.572	24.94	0.8806	<b>88.06</b>
	9	37.87	133.4	128.1	1.459	2.144	18.69	0.9105	<b>91.05</b>
	11	27.17	122.9	117.6	1.772	2.425	13.41	0.9358	<b>93.58</b>
2	1	166.1	205.7	143.7	1.872	2.394	75.85	0.6076	<b>60.76</b>
	3	140.9	168.0	131.0	1.996	2.453	64.35	0.6671	<b>66.71</b>
	5	123.4	134.3	122.8	1.803	1.598	56.32	0.7085	<b>70.85</b>
	7	86.32	136.4	129.2	1.133	2.422	39.42	0.7961	<b>79.61</b>
	9	54.66	201.4	133.3	2.019	3.312	24.96	0.8709	<b>87.09</b>
	11	36.80	77.30	57.74	2.024	3.061	16.80	0.9131	<b>91.31</b>
3	1	144.3	129.5	119.0	1.550	2.667	71.22	0.6591	<b>65.91</b>
	3	118.9	132.9	127.2	1.490	1.492	58.68	0.7191	<b>71.91</b>
	5	94.35	139.3	133.8	1.462	2.631	46.56	0.7772	<b>77.72</b>
	7	82.96	170.5	128.2	2.044	3.074	40.94	0.8040	<b>80.40</b>
	9	70.72	129.9	113.7	2.869	2.438	34.90	0.8329	<b>83.29</b>
	11	56.07	119.4	117.4	1.123	2.901	27.67	0.8675	<b>86.75</b>

The causality factors CF-2 and CF-3 in Table 7 are very close to theoretical values that according to EFM theory [61] should guarantee the validity of Tafel slopes and corrosion current densities. Values of causality factors in Table 7 indicates that the measured data are of good quality. The standard values for CF-2 and CF-3 are 2 and 3, respectively. The causality factor is calculated from the frequency spectrum of the current response. If the causality factors are approximately equal to the predicted values of 2 and 3, there is a causal relationship between the perturbation signal and the response signal. Then the data are assumed to be reliable [30]. When CF-2 and CF-3 are in the range 0-

2 and 0-3, respectively, then the EFM data is valid. The deviation of causality factors from their ideal values might due to that the perturbation amplitude was too small or that the resolution of the frequency spectrum is not high enough also another possible explanation that the inhibitor is not performing very well [31]. The inhibition efficiencies %IE<sub>EFM</sub> increase by increasing the studied extract concentrations for either copper or brass and was calculated as follows:

$$\%IE_{EFM} = \left(1 - \frac{i_{corr}}{i_{corr}^0}\right) \times 100 \tag{13}$$

where  $i_{corr}^0$  and  $i_{corr}$  are corrosion current densities in the absence and presence of investigated compounds, respectively.

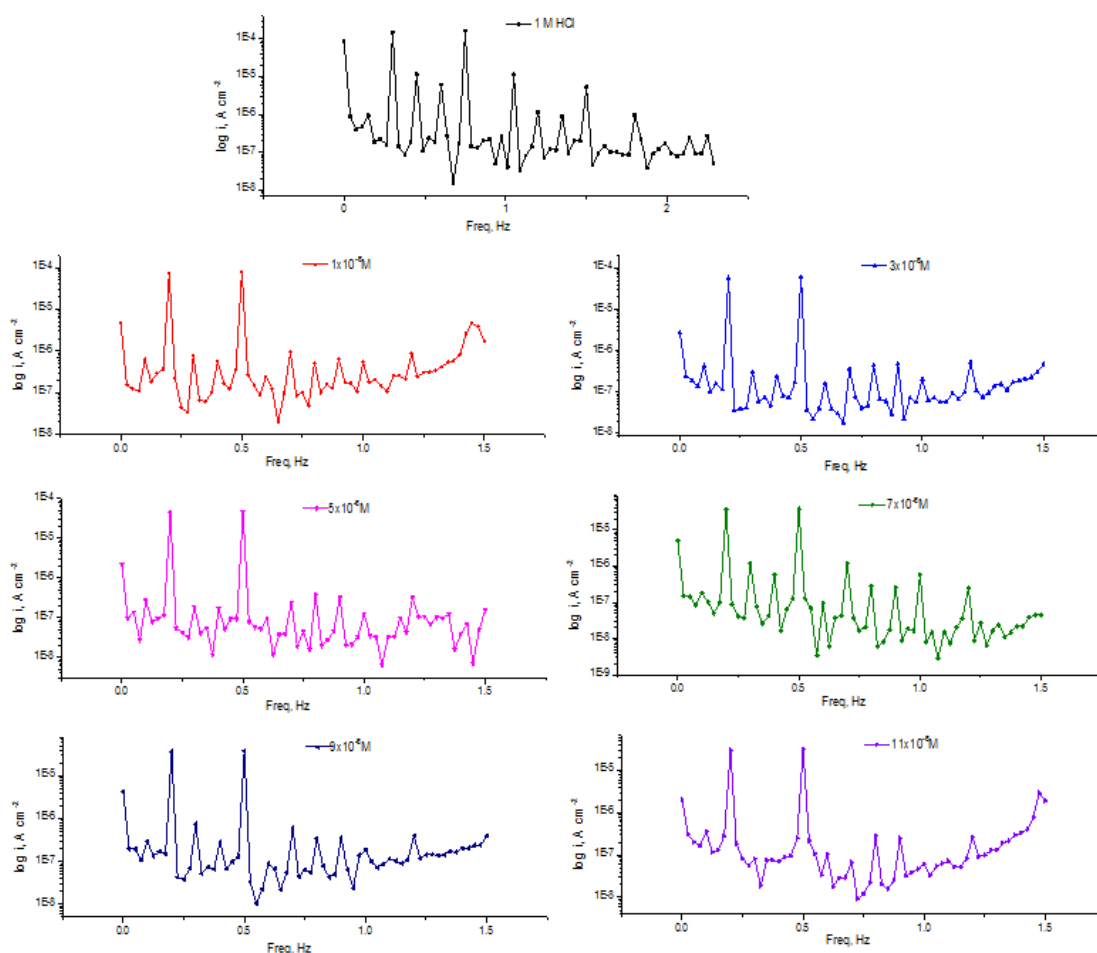


**Figure 10.** EFM spectra for C-steel in 1.0 M HCl in the presence of different concentrations of compound (1) at 25° C

### 3.7. SEM/EDX examination

The scanning electron microscope images and energy dispersive X-ray analysis further supported the formation of a surface film by the inhibitors and their interaction with surface atoms of carbon steel.

Figure 11a illustrates the morphology of the surface of polished carbon steel electrode before exposure to corrosion media (blank). The specimens were subjected to microscopic examination at x 500. The micrograph shows a characteristic inclusion, which was probably an oxide inclusion. Figure 11b shows SEM image of the surface of the studied carbon steel electrode specimen after immersion in 1.0 M HCl solution for 24 h. The micrograph reveals that the surface was strongly damaged. The corroded areas are shown as black grooves in the specimen with gray and white zones, which correspond to the dandruff of iron oxide. It suggested an uncovered surface of metal electrode severally corroded.

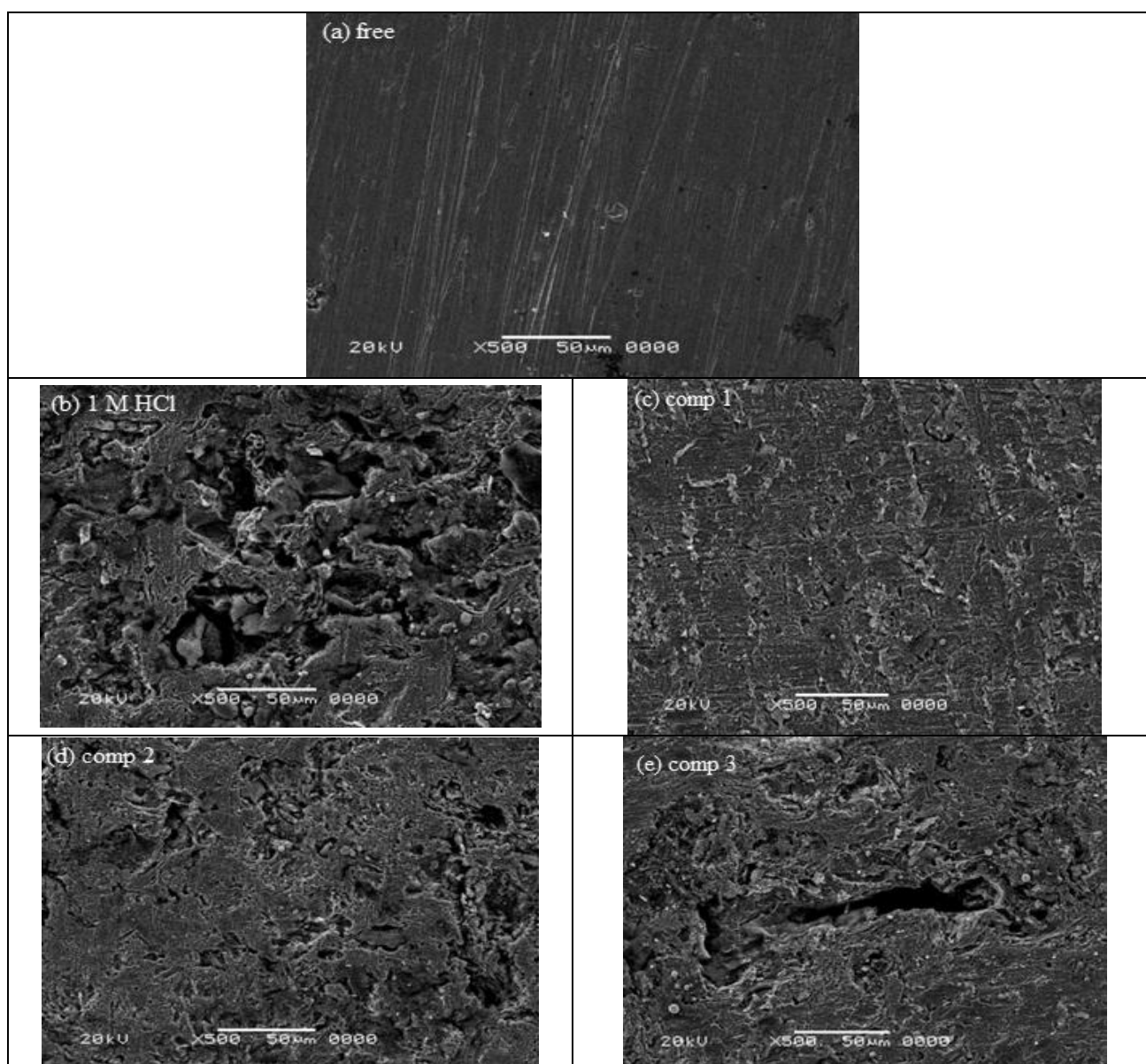


**Figure 11.** SEM micrographs of carbon steel surface (a) before of immersion in 1.0 M HCl, (b) after 24 h of immersion in 1 M HCl and (c-e) after 24 h of immersion in 1 M HCl +  $11 \times 10^{-6}$  M of chalcone derivatives at 25°C

The highly oxidized phase has perhaps been formed in air when desiccated under no protection for the surface. Figures 11(c-e) show SEM images for the surface of another carbon steel specimen after immersion for the same time interval in 1.0 M HCl solution containing  $11 \times 10^{-6}$  M from organic compounds. The micrograph reveals that the inhibited metal surface is smoother than the uninhibited surface, a good protective film present on the metal surface. This confirms the highest inhibition efficiency of the inhibitors.

It is important to take into consideration the percentage of the elements present on the surface of the carbon steel (Table 8).

**Table 8.** Surface composition (wt %) of carbon steel before and after immersion in 1.0 M HCl without and with  $11 \times 10^{-6}$  M of chalcone derivatives at 25 °C.

(Mass %)	Fe	Mn	Si	P	O	N	Cl
<b>Free</b>	98.890	1.060	0.173	0.035	-	-	-
<b>1 M HCl</b>	97.450	1.050	0.477	0.200	0.990	-	-
<b>1</b>	68.700	0.813	-	-	20.227	10.123	0.100
<b>2</b>	84.980	1.030	0.115	-	13.76	-	0.115
<b>3</b>	73.000	0.837	0.230	-	11.823	14.027	0.082

### 3.8. Mechanism of inhibition

Most organic inhibitors contain at least one polar group with an atom of nitrogen or sulphur or in some cases selenium and phosphorus. The inhibiting properties of many compounds are determined by the electron density at the reaction center [62]. With increase in electron density in the center, the chemisorption between the inhibitor and the metal are strengthened [63]. From the observations drawn from the different methods, corrosion inhibition of C-steel in acid chloride solution by the investigated inhibitors as indicated from weight loss, potentiodynamic polarization, EIS and EFM techniques was found to depend on the concentration and the nature of the inhibitor. The adsorption of organic molecules on the solid surfaces cannot be considered only as purely physical or as purely chemical adsorption phenomenon. In addition to the chemical adsorption, inhibitor molecules can also be adsorbed on the steel surface via electrostatic interaction between the charged metal surface and charged inhibitor molecule if it is possible. The free energy of adsorption value is not very greater than  $-40 \text{ kJ mol}^{-1}$  should indicate contribution of physical adsorption. If the contribution of electrostatic interactions takes place, the following adsorption process can additionally be discussed. The investigated compounds have basic character and expected to be protonated in equilibrium with the corresponding neutral form in strong acid solutions. Because C-steel surface carried positive charge,  $\text{Cl}^-$  ions should be first adsorbed onto the positively charged metal surface. Then the inhibitor molecules adsorb through electrostatic interactions between the negatively charged metal surface and positively charged inhibitor molecule and form a protective layer. In this way, the oxidation reaction of Fe can be prevented [64]. The protonated inhibitors molecules are also adsorbed at cathodic sites of

metal in competition with hydrogen ions. The adsorption of protonated inhibitors molecules reduces the rate of hydrogen evolution reaction [65].

Compound (1) contains dimethyl amine group in the para position ( $\sigma_p = -0.88$ ). This group acts as electron donating group which increase the electron density of the ring and increase the ability of the inhibitor to be adsorbed on the metal surface. So, compound (1) is the highest effective one. Compound (2) comes after compound (1) in inhibition efficiency because it contains H-atom with  $\sigma_p = 0.0$  which does not contribute any charge density to the molecule. Compound (3) is the least effective one due to the presence of  $\text{NO}_2$  group in the para position with  $\sigma_p = +0.78$  which is electron withdrawing group. The presence of this group will decrease the electron density on the molecule.

#### 4. CONCLUSIONS

From the overall experimental results the following conclusions can be deduced:

Chalcone derivatives are good inhibitors and act as mixed type inhibitors for carbon steel corrosion in 1.0 M HCl solution. The results obtained from all measurements showed that the inhibiting action increases with the inhibitors concentration and decreases with the increasing in temperature. Double layer capacitances decrease with respect to blank solution when chalcone derivatives are added. This fact confirms the adsorption of the investigated compounds molecules on the carbon steel surface. The adsorption of chalcone derivatives on the carbon steel surface at different temperature was found to obey the Langmuir adsorption isotherm and this adsorption is physisorption. The values of inhibition efficiencies obtained from the different independent quantitative techniques used show the validity of the results.

#### References

1. S. Bilgiç, *Mater. Chem. Phys.* 70 (2002) 52.
2. F. Bentiss, M. Traisnel, M.Lagrenée, *Corros. Sci.* 42 (2000) 127.
3. M.A. Quraishi, M.A.W. Khan, M. Ajmal, *Corrosion* 53 (1997) 475.
4. E. Khamis, *Corrosion*. 46 (1990) 476.
5. A. Afidah, E. Rahim, J. Rocca, *Corros. Sci.* 49 (2007) 402.
6. A.S. Fouda, A.A. Al-Sharawy, E.E. El-Katori, *Desalination* 201 (2006) 1.
7. H.L. Wang, H.B. Fan, J.S. Zheng, *Mater. Chem. Phys.* 77 (2002) 655
8. J. I. Bhat, V. D. P. Alva, *J. Korean. Chem. Soc.* 55 (2011) 835.
9. A.S. Fouda, Y.A. Elewady, H.K. Abd El-Aziz, A.M. Ahmed, *Int. J. Electrochem. Sci.*, 7 (2012) 10456.
10. A.S. Fouda, A.M. El-desoky, D.M. Ead, *Int. J. Electrochem. Sci.*, 8 (2013) 8823
11. E.-S.M. Sherif, A.A. Almajid, *J. Appl. Electrochem.*, 40(2010)1555.
12. K. Shalabi, A.S. Fouda, G.Y. Elewady, A. Elaskalany, *Protection of Metals and Phys. Chem. Surfs.*, 50(3)(2014)420
13. A.S. Fouda, H.E. Megahed, T. Younis, Sh. Abd El-Salam, E.-S.M. Sherif, *Protection of Metals and Phys. Chem. Surfs.*, 50(2)(2014)254
14. E.-S.M. Sherif, R.M. Erasmus, J.D. Comins, *Journal of Colloid and Interface Science*, vol. 306, pp. 96-104, 2007.

15. E.-S.M. Sherif, R.M. Erasmus, J.D. Comins, *J. Coll. Interface Sci.*, 309 (2007) 470.
16. E.-S.M. Sherif, R.M. Erasmus, J.D. Comins, *J. Coll. Interface Sci.*, 311(2007)144.
17. E.S.M. Sherif, R.M. Erasmus, J.D. Comins, *J. Appl. Electrochem.*, 39 (2009) 83
18. E.S.M. Sherif, R.M. Erasmus, J.D. Comins, *Corros. Sci.*, 50(2008) 3439.
19. E.M. Sherif, S.-M. Park, *Electrochim. Acta*, 51(2006) 6556.
20. E.M. Sherif, S.-M. Park, *Corros. Sci.*, 48(2006) 4065.
21. E.-S.M. Sherif, *Appl. Surf. Sci.*, 252(2006) 8615.
22. E.-S.M. Sherif, *Int. J. Electrochem. Sci.*, 6(2011) 3077
23. E.-S.M. Sherif, *Int. J. Electrochem. Sci.*, 6 (2011) 5372.
24. E.-S.M. Sherif, A.H. Ahmed, Reactivity in Inorg., *Metal-Org., and Nano- Metal Chem.*, 40(2010) 365
25. E.S.M. Sherif, *Solid State Electrochem.*, 16(2012) 891.
26. E.S.M. Sherif, *Mater. Chem. Phys.* 129 (2011) 961.
27. E.S.M. Sherif, *J. Mater. Eng. Perform.*, 19(2010) 873.
28. O.L. Riggs Jr., C.C. Nathan (Ed.), *Corrosion Inhibitors*, 2nd ed., NACE, Houston, TX, 1973.
29. T. Narendar, K. Papi Reddy, *Tetrahedron Letters* 48 (2007) 3177.
30. R. W. Bosch, J. Hubrecht, W. F. Bogaerts, B. C. Syrett, *Corrosion* 57 (2001) 60.
31. S.S. Abdel- Rehim, K.F. Khaled, N.S. Abd-Elshafi, *Electrochim. Acta*, 51 (2006) 3269.
32. M. Abdallah, *Corros. Sci.* 46 (2004) 1981.
33. I. Langmuir, *J. Am. Chem. Soc.*, 39 (1917) 1848.
34. J. I. Bhat, V. D. P. Alva, *J. Korean. Chem. Soc.* 55 (2011) 835-841.
35. E. E. Oguzie, B. N. Okolue, E. E. Ebenso, G. M. Onuoha, A. I. Onuchukwu, *Mater. Chem. Phys.* 87 (2004) 394.
36. A. Popova, E. Sokolova, S. Raicheva, M. Chritov, *Corros. Sci.* 45 (2003) 33.
37. Z. Szlarska-Smialowska, J. Mankowski, *Corros. Sci.*, 18 (1978) 953.
38. A. Yurt, S. Ulutas, H. Dal, *Appl. Surf. Sci.* 253 (2006) 919.
39. T.P. Zhao, G.N. Mu, *Corros. Sci.* 41(1999) 1937.
40. A. Döner, G. Kardas, *Corros. Sci.* 53 (2011) 4223.
41. B.G. Ateya, B.E. El-Anadouli, F.M. El-Nizamy, *Corros. Sci.* 24 (1984) 509.
42. X.H. Li, S.D. Deng, H. Fu, G.N. Mu, *Corros. Sci.* 52 (2010) 1167.
43. J.O.M. Bochrus, A.K. N. Reddy, *Modern Electrochemistry*, New York: Plenum Press, 1970.
44. S. Martinez, I. Stern, *Appl. Surf. Sci.* 199 (2002) 83-89.
45. K. Tebbji, I. Bouabdellah, A. Aouniti, B Hammouti, H. Oudda, M. Benkaddour , A. Ramdani, *Mater. Lett.* 61 (2007) 799.
46. M. Mihit, S. El-Issami, M. Bouklah, L. Bazzi, B. Hammouti, E.A. Addi, R. Salghi , S. Kertit, *Appl. Surf. Sci.* 252 (2006) 2389.
47. M. Bouklah, B. Hammouti, M. Lagrenee , F. Bentiss, *Corros. Sci.* 48 (2006) 2831.
48. M. Bouklah , N. Benchat., B. Hammouti, A. Aouniti , S. Kertit, *Mater. Lett.* 60 (2006) 1901.
49. S.S. Abd El-Rehim, M.A.M Ibrahim, K.F. Khaled, *J. Appl. Electrochem.* 29 (1999) 593.
50. M. Abdallah, *Corros. Sci.* 45 (2003) 2705.
51. K. Shalabi, Y.M. Abdallah, H. M. Hassan, A.S. Fouda, *Int. J. Electrochem. Sci.*, 9 (2014) 1468.
52. Z.H. Tao, S.T. Zhang, W.H. Li , B.R. Hou, *Corros. Sci.* 51 (2009) 2588.
53. E.S. Ferreira, C. Giacomelli, F.C. Giacomelli , A. Spinelli, *Mater. Chem. Phys.* 83 (2004) 129.
54. M. Behpour, S.M. Ghoreishi, N. Mohammadi, N. Soltani , M. Salavati-Niasari, *Corros. Sci.* 52 (2010) 4046.
55. L. Larabi, Y. Harek, M. Traianel , A. Mansri, *J. Appl. Electrochem.* 34 (2004) 833.
56. M. Lebrini, M. Lagrenee, H. Vezin, M. Traisnel, F. Bentiss, *Corros. Sci.* 49 (2007) 2254.
57. S. Martinez, M. Metikoš-Hukovic, *J. Appl. Electrochem.* 33 (2003) 1137.

58. J.L. Trinstancho-Reyes, M. Sanchez-Carrillo, R. Sandoval-Jabalera, V.M. Orozco-Carmona, F. Almeraya-Calderon, J.G. Chacon-Nava, J.G. Gonzalez-Rodriguez , A. Martínez-Villafane, *Int. J. Electrochem. Sci.*, 6 (2011) 419.
59. C.S. Hsu , F. Mansfeld, *Corrosion* 57 (2001) 747.
60. F. Bentiss, M. Bouanis, B. Mernari, M. Traisnel, H. Vezin , M. Lagrenee, *Appl. Surf. Sci.*, 253 (2007) 3696.
61. R.R. Anand, R.M. Hurd, N. Hackerman, *J. Electrochem. Soc.* 112(1965) 138.
62. E.L. Cook, N. Hackerman, *J. Phys. Chem.* 55 (1951) 549.
63. J.J. Bordeaux, N. Hackerman, *J. Phys. Chem.* 61 (1957) 1323.
64. H. Keles, M. Keles, I. Dehri , O. Serindag, *Mater. Chem. Phys.* 112 (2008) 173.
65. A. Yurt, A. Balaban, S. Ustün Kandemir, G. Bereket, B. Erk, *Mater. Chem. Phys.*, 85 (2004) 420.

© 2014 The Authors. Published by ESG ([www.electrochemsci.org](http://www.electrochemsci.org)). This article is an open access article distributed under the terms and conditions of the Creative Commons Attribution license (<http://creativecommons.org/licenses/by/4.0/>).